Supplement of Atmos. Chem. Phys., 16, 12875–12896, 2016
http://www.atmos-chem-phys.net/16/12875/2016/
doi:10.5194/acp-16-12875-2016-supplement


Atmospheric Chemistry and Physics

*Supplement of*

# Variations in the chemical composition of the submicron aerosol and in the sources of the organic fraction at a regional background site of the Po Valley (Italy)

**Michael Bressi et al.**

*Correspondence to:* Michael Bressi (michael.s.bressi@gmail.com), Claudio A. Belis (claudio.belis@jrc.ec.europa.eu), and Fabrizia Cavalli (fabrizia.cavalli@jrc.ec.europa.eu)

## S1. Ammonium nitrate and sulfate calibrations

Ammonium nitrate calibrations were performed at least once every season following the procedure described by Aerodyne (2010); results are presented in Figure S2. Although noticeable discrepancies are observed when comparing $RF_{NO_3}$ values season by season - e.g. 3.8E-11±2.0E-12 and 2.7E-11±4.0E-13 amp/(µg/m$^3$) during April and June, respectively, for ACSM#1 - , Figure S2 suggests that these differences are not attributable to a seasonal behaviour of the instrument but instead represent the uncertainties associated with the calibration procedure (related to e.g. the aerosol generator, the DMPS flow or the relative humidity of the generated particles). Thus, for several-months campaigns with an ACSM, we suggest using an average nitrate response factor determined by the slope of all plotted calibration points, independently of the calibration (Figure S2). We also suggest using an average ammonium RIE, which can be calculated as the average of every seasonal calibration (i.e. average of the slopes) since y-intercepts differ from one calibration to the other, likely due to the lower sensitivity of the instrument to ammonium-related fragments (e.g. *m/z* 17 and 16 from $NH_3^+$ and $NH_2^+$, respectively) for which interferences with water and air fragments ($HO^+$ and $O^+$, respectively) are usually observed (Ng et al., 2011a). The resulting $RIE_{NH4}$ are 5.8±0.1 and 6.5±1.0 for ACSM#1 and #2, respectively, which is in the 3.2-14.7 range reported in Crenn et al. (2015) from an inter-ACSM comparison. Sulfate RIEs ($RIE_{SO4}$) are calculated similarly to $RIE_{NH4}$ when ammonium sulfate (AS) calibrations are performed. A literature-based $RIE_{SO4}$ value of 1.15 (Canagaratna et al., 2007) was applied to ACSM#1 since the custom scan file later developed by Aerodyne for AS calibration was not available yet; two attempts to experimentally determine $RIE_{SO4}$ on ACSM#1 were however made by injecting one AS solution of a given concentration using the AN tool similarly to what is described by Aerodyne (2010), which led to an approximate average $RIE_{SO4}$ of 1.25±0.23 i.e. to experimental values that are comparable to the aforementioned literature one. An experimentally determined $RIE_{SO4}$ value of 0.6±0.1 was applied to ACSM#2 based on two AS calibrations performed following Aerodyne (2013) using 5-10 solutions ranging from 0 to 15 µg/m$^3$.

## S2. Source apportionment configurations

*Constrained factor profiles set up*

Unconstrained PMF allowed for the identification of an HOA-like factor (with high *m/z* 55 and 57), a BBOA-like factor (with high *m/z* 60 and 73, except for summer where BBOA was not found) and an OOA-like factor (with high *m/z* 44 and 43). However, the BBOA factor profile was not fully satisfactory since specific fragments (e.g. *m/z* 43 and 44, Figure S4) were missing, contrary to what is reported in the literature for primary BBOA emissions (Heringa et al., 2011). Constraining the HOA factor only, with low *a*-values (0.05; Crippa et al., 2014) leads to solutions with high seed variability indicating unstable results. Constraining the BBOA factor only with relatively high *a*-values (0.3-0.5; Crippa et al., 2014) does not allow an HOA factor to be identified (factor with high m/z 44 and 60), and leads to unsatisfactory BBOA time series (which are similar to HOA time series when HOA is constrained). Constraining both HOA and BBOA factors leads to satisfactory solutions with relevant factor profiles, time series and daily cycles that will be discussed later on. Note that an attempt to constrain a COA factor was also made, since it has been reported to be an important source of OA (10-30%) in urban areas widely (e.g. Allan et al., 2010; Huang et al., 2010; Mohr et al., 2012; Sun et al., 2011). No clear evidence indicates the presence of COA from our dataset as it is suggested by i) the absence of lunch and dinner peaks for constrained COA factor contributions, ii) the position of our data in the $f_{55}$ to $f_{57}$ scatter plot suggested by Mohr et al. (2012) (slope closer to HOA-like aerosols) and iii) the dubiously high COA and low HOA relative contributions to OA (13 and 7% on average, respectively) when constraining COA. The absence of a COA factor in our study might be related to i) high similarities existing between HOA and COA unit mass resolution factor profiles, ii) lower sensitivity, time- and mass-to-charge-resolution of the ACSM compared with the (high-resolution time-of-flight-) AMS used in the aforementioned studies, iii) the type of site studied here (rural), which is likely less influenced by local cooking emissions than urban sites, but which could instead be impacted by aged, processed COA particles emitted in urban areas that would then undergo oxidative processes during their transport leading to OOA-like aerosols. Further discussion on the presence (or absence) of cooking factors at rural sites of the Po Valley can be found in Dall'Osto et al. (2015).

*Identification of the optimal number of factors*

Solutions applying various numbers of factors and constraining different factor profiles for each season are summarized in Table S1. During summer, the optimal solution is found with two factors, which allows for the identification of HOA and OOA (OOA-2F). Setting three factors splits OOA-2F into SV-OOA and LV-OOA like factors as suggested by their factor profiles and daily cycles. However, the absence of *m/z* 57 in SV-OOA contrary to what is reported in the literature (Ng et al., 2011b), the high correlation observed between SV-OOA and HOA ($r^2$=0.67) and the poor correlation observed with nitrate ($r^2$=0.13) highlights the limitations of this SV-OOA factor. During summer, the HOA and OOA 2-factor solution was thus preferred, considering that OOA is here likely influenced by both SV- and LV-OOA. During spring, autumn and winter, the optimal solution is found with three factors, which allows for the identification of HOA, BBOA and OOA. Setting two factors leads to an HOA factor, and a mixing of BBOA and OOA in a single factor, as it is attested by the presence of high $f_{43}$, $f_{44}$, $f_{55}$, $f_{57}$, $f_{60}$ and $f_{73}$ in the latter. Choosing four factors splits the initial OOA (OOA-3F) into two OOA factors (OOA1-4F and OOA2-4F), for which mass spectra and time series vary depending on the season studied. In general, OOA1-4F is similar to OOA-3F in terms of factor profile and time series, whereas OOA2-4F presents biomass burning characteristics (high $f_{60}$ and $f_{73}$, correlations with BBOA, etc.) in addition to typical OOA features (high $f_{44}$). However, this second OOA2-4F factor cannot be clearly interpreted as an OOA-BBOA factor as it has previously been reported (e.g. Crippa et al., 2013), due to the absence of key mass fragments during Spring and Autumn (e.g. *m/z* 29, Alfarra et al., 2007), or higher correlations with primary factors than secondary compounds during winter (see Table S1). During spring, autumn and winter, we therefore chose the HOA, BBOA and OOA 3-factors solution, keeping in mind that OOA is likely influenced by secondary BBOA here.

*Identification of the appropriate a-value*

The influence of *a*-values on the apportionment of organics has been investigated. Different scenarios were tested applying very low to very high constraints to HOA and BBOA factors (see Table S2 for more details). Solutions were defined as relevant or not depending on the seed variability, factor daily cycles, the independence of factor contributions, etc.  They were then compared by investigating i) variations of the seasonal average contribution of each factor and ii) factor time series correlations with independent measurements. Results are summarized in Table S2 and Figure S5. In general, very low and very high constraints lead to irrelevant solutions (e.g high seed variability, traffic peaks for BBOA, etc.) for which the average contributions of each factor vary substantially from other scenarios (e.g. see very high constraint during winter). Low to high constraints results in comparable solutions in terms of both relative contributions and correlations with external measurements. We decided to apply low constraints (i.e. *a*-values of 0.1 and 0.5 for HOA and BBOA, respectively) to give as much freedom as possible to our factor profiles while remaining in the range of plausible solutions. Correlations with independent measurements are further discussed in Sect. 3.2 of the manuscript.

*Set up of the period duration*

Choosing the appropriate period duration for source apportionment (SA) analysis demands a compromise between i) including as many data as possible to reach robust and statistically significant solutions and ii) limiting this amount of data to respect the assumption that factor profiles are constant during the studied period. In our study, SA was performed on three period durations: i) the entire year, ii) two 6-months periods and iii) four distinct seasons. Comparable solutions are found for the three different configurations with the identification of reasonable (factor profile, diurnal cycle, comparison with external data) HOA, BBOA and OOA factors. However, when performing SA on the entire year and on 6-months periods i) the HOA factor does not exhibit a clear morning (i.e. traffic) peak and ii) the ME-2 assumption that factor profiles are constant during a studied period becomes questionable. Note that in the 1-year and 6-months configurations, BBOA represents 3 and 4% of OA during summer, respectively, which can be viewed as an upper estimate of agricultural waste burning contributions. In addition, performing SA on a seasonal basis allows the seasonal variability of factor profiles to be captured (e.g. higher contribution of $f_{60}$ in OOA during winter). We thus preferred interpreting SA results based on seasonal experiments, although comparable conclusions would be reached with the 6-months and one-year configurations.

## S3. Errors in the estimation of elemental ratios

The errors (average absolute value of the relative error) are estimated to be 28%, 8% and 13% for O/C, OM/OC and H/C for standard molecules, respectively, and 0.06 units for OSc (Canagaratna et al., 2015). Discrepancies in $f_{44}$ quantifications between different ACSMs, and between ACSMs and AMS (Crenn et al., 2015; Fröhlich et al., 2015) are however likely to increase the uncertainties associated with O/C, OM/OC and OSc estimates. In particular, in the abovementioned inter-instrument comparison, ACSMs have been reported to overestimate $f_{44}$ by up to a factor of 2 compared to the HR-ToF-AMS (Fröhlich et al., 2015). Comparisons with studies using (HR-ToF-) AMS instruments will thus not be reported and only variations within this dataset will be discussed. Regarding the two ACSMs used in this study, absolute differences between median estimates from two-months co-located measurements in summer are 0.05, 0.07, 0.07 and 0.17 for O/C, OM/OC, H/C and OSc, respectively (see Figure S8).

## S4. Seasonal characteristics of fine aerosol pollution events

The seasonal variations of NR-$PM_1$ chemical composition and OA factors' contributions as a function of total NR-$PM_1$ mass is shown in Fig. S9. During spring and autumn, the characteristics of submicron aerosol pollution events are similar to what is described on the annual scale (Sect. 4.3). Nitrate and BBOA are the main responsible for NR-$PM_1$ concentrations increase. Specific patterns are observed during summer, with i) fairly stable contributions of OA sources irrespective of NR-$PM_1$ levels, and ii) noticeable proportions of sulfate (~20%). Sulfate is nevertheless not responsible for the increase of NR-$PM_1$ concentrations. Note that the intensity and frequency of NR-$PM_1$ pollution events are lower during summer compared to other seasons. Finally, the importance of BBOA in submicron aerosol pollution events is highlighted during winter ([BBOA]~40% of [OA], when [NR-$PM_1$]> 30 $\mu g/m^3$). An increase of

HOA is for the first time observed during this season, which indicates that primary sources largely contribute to high NR-$PM_1$ concentrations during winter.

Table S1. Tests to identify the optimal number of factors.

| Season | Number of factors | Factors fixed | Factors identified | Comments |
|---|---|---|---|---|
| Spring | 2 | HOA | HOA, OOA mixed | OOA mixed with primary BBOA |
| | **3** | **HOA, BBOA** | **HOA, BBOA, OOA** | **Optimal solution** |
| | 4 | HOA, BBOA | HOA, BBOA, OOA1, OOA2 | OOA1 factor not fully satisfactory: high time series correlation with BBOA factor ($r^2$=0.74) suggesting an OOA-BBOA factor but discrepancies with already-found OOA-BBOA factor profile in the literature (e.g. *m/z* 17, 29, 41) |
| | 5 | HOA, BBOA | Factors split | High correlations between factor profiles and time series |
| Summer | **2** | **HOA** | **HOA, OOA** | **Optimal solution** |
| | 3 | HOA | HOA, LV-OOA like, SV-OOA like | High seed variability. SV-OOA factor not fully satisfactory: no *m/z* 57, high time series correlations with HOA ($r^2$=0.67), poor correlation with nitrate ($r^2$=0.13) |
| | 3 | HOA, BBOA | HOA, BBOA, OOA | High contribution of BBOA compared to HOA (22 and 7% of OA, respectively) which is very unlikely in summer |
| | 4 | HOA | Factors split | High correlations between factor profiles and time series |
| Autumn | 2 | HOA | HOA, OOA mixed | OOA mixed with primary BBOA |
| | **3** | **HOA, BBOA** | **HOA, BBOA, OOA** | **Optimal solution** |
| | 4 | HOA, BBOA | HOA, BBOA, OOA1, OOA2 | OOA1 factor not fully satisfactory: high profile correlations with OOA2 factor ($r^2$=0.97), high time series correlation with BBOA ($r^2$=0.69) suggesting an OOA-BBOA factor but discrepancies with already-found OOA-BBOA factor profile in the literature (e.g. *m/z* 17, 29) |
| | 5 | HOA, BBOA | Factors split | High correlations between factor profiles and time series |
| Winter | 2 | HOA | HOA, OOA | OOA mixed with primary BBOA |
| | **3** | **HOA, BBOA** | **HOA, BBOA, OOA** | **Optimal solution** |
| | 4 | HOA, BBOA | HOA, BBOA, OOA1, OOA2 | OOA1 factor not fully satisfactory: time series correlation with primary factors such as HOA ($r^2$=0.72) and BBOA ($r^2$=0.70), but poor correlations with secondary compounds such as $NO_3$ ($r^2$=0.22) or $SO_4$ ($r^2$=0.12) |
| | 5 | HOA, BBOA | Factors split | High correlations between factor profiles and time series |

Table S2. Influences of *a*-values on the relative contribution of each factor and the agreement with specific *m/z* or independent measurements. Constraints are defined as: very low: *a*-values calculated for every *m/z* from the relative standard deviation of reference factor profiles; low: $a_{HOA}$=0.10, $a_{BBOA}$=0.50; intermediate: $a_{HOA}$=0.075, $a_{BBOA}$=0.40; high: $a_{HOA}$=0.05, $a_{BBOA}$=0.30; very high: $a_{HOA}$=0, $a_{BBOA}$=0. Note that *a*-values used from low to high constraints are chosen following the empiric recommendations of Crippa et al. (2014).

| | | | HOA | | | | | | BBOA | | | | | | OOA | | | | | |
|---|---|---|---|---|---|---|---|---|---|---|---|---|---|---|---|---|---|---|---|---|
| | | | Contribution | $r^2$ | | | | | Contribution | $r^2$ | | | | | Contribution | $r^2$ | | | | |
| | Constraint | Relevance of solution | % | Org_67 | Org_81 | NOx | CO | BC | % | Org_60 | Org_73 | NOx | CO | BC | % | Org_43 | Org_44 | NH4 | SO4 | NO3 |
| SPRING | very low | Not relevant | 13 | 0.27 | 0.23 | 0.00 | 0.00 | 0.14 | 32 | 0.98 | 0.95 | 0.31 | 0.78 | 0.66 | 55 | 0.88 | 0.97 | 0.79 | 0.43 | 0.81 |
| | low | Relevant | 9 | 0.60 | 0.55 | 0.03 | 0.08 | 0.28 | 32 | 0.99 | 0.97 | 0.32 | 0.81 | 0.70 | 59 | 0.78 | 0.67 | 0.76 | 0.43 | 0.77 |
| | intermediate | Relevant | 8 | 0.52 | 0.46 | 0.02 | 0.05 | 0.24 | 31 | 0.99 | 0.96 | 0.31 | 0.80 | 0.69 | 61 | 0.89 | 0.95 | 0.75 | 0.43 | 0.77 |
| | high | Relevant | 8 | 0.42 | 0.36 | 0.01 | 0.02 | 0.18 | 29 | 0.98 | 0.96 | 0.31 | 0.79 | 0.67 | 64 | 0.92 | 0.96 | 0.75 | 0.40 | 0.77 |
| | very high | Not relevant | 7 | 0.83 | 0.80 | 0.19 | 0.43 | 0.56 | 25 | 0.90 | 0.92 | 0.24 | 0.69 | 0.64 | 64 | 0.91 | 0.98 | 0.79 | 0.40 | 0.81 |
| SUMMER | very low | Acceptable | 22 | 0.93 | 0.95 | 0.07 | 0.42 | 0.56 | | | | | | | 78 | 0.94 | 0.94 | 0.56 | 0.63 | 0.18 |
| | low | Relevant | 14 | 0.90 | 0.91 | 0.07 | 0.40 | 0.52 | | | | | | | 86 | 0.97 | 0.94 | 0.54 | 0.60 | 0.19 |
| | intermediate | Relevant | 13 | 0.89 | 0.91 | 0.07 | 0.40 | 0.51 | | | - | | | | 87 | 0.97 | 0.92 | 0.54 | 0.60 | 0.19 |
| | high | Relevant | 13 | 0.89 | 0.91 | 0.07 | 0.40 | 0.51 | | | | | | | 87 | 0.97 | 0.93 | 0.54 | 0.60 | 0.19 |
| | very high | Relevant | 12 | 0.88 | 0.90 | 0.07 | 0.39 | 0.50 | | | | | | | 88 | 0.97 | 0.91 | 0.54 | 0.59 | 0.19 |
| AUTUMN | very low | Acceptable | 15 | 0.43 | 0.39 | 0.02 | 0.01 | 0.13 | 23 | 0.97 | 0.97 | 0.07 | 0.67 | 0.48 | 63 | 0.77 | 0.94 | 0.53 | 0.57 | 0.42 |
| | low | Relevant | 11 | 0.63 | 0.61 | 0.07 | 0.10 | 0.24 | 21 | 0.99 | 0.97 | 0.06 | 0.68 | 0.47 | 68 | 0.82 | 0.92 | 0.47 | 0.53 | 0.38 |
| | intermediate | Relevant | 11 | 0.58 | 0.55 | 0.06 | 0.07 | 0.20 | 21 | 0.99 | 0.97 | 0.06 | 0.68 | 0.47 | 69 | 0.81 | 0.92 | 0.47 | 0.54 | 0.38 |
| | high | Relevant | 10 | 0.56 | 0.53 | 0.06 | 0.06 | 0.20 | 21 | 0.98 | 0.97 | 0.06 | 0.67 | 0.47 | 68 | 0.80 | 0.91 | 0.47 | 0.55 | 0.37 |
| | very high | Not relevant | 11 | 0.84 | 0.85 | 0.11 | 0.35 | 0.45 | 22 | 0.86 | 0.91 | 0.06 | 0.62 | 0.50 | 67 | 0.82 | 0.95 | 0.51 | 0.52 | 0.43 |
| WINTER | very low | Relevant | 11 | 0.76 | 0.75 | 0.41 | 0.51 | 0.55 | 37 | 0.97 | 0.97 | 0.20 | 0.66 | 0.63 | 52 | 0.79 | 0.98 | 0.51 | 0.42 | 0.66 |
| | low | Relevant | 11 | 0.58 | 0.57 | 0.34 | 0.33 | 0.39 | 36 | 0.98 | 0.97 | 0.20 | 0.66 | 0.63 | 53 | 0.80 | 0.99 | 0.50 | 0.39 | 0.66 |
| | intermediate | Relevant | 11 | 0.51 | 0.49 | 0.32 | 0.29 | 0.35 | 35 | 0.97 | 0.97 | 0.20 | 0.65 | 0.62 | 54 | 0.80 | 0.99 | 0.50 | 0.39 | 0.66 |
| | high | Relevant | 11 | 0.59 | 0.58 | 0.37 | 0.36 | 0.42 | 37 | 0.97 | 0.97 | 0.20 | 0.65 | 0.62 | 53 | 0.80 | 0.99 | 0.50 | 0.39 | 0.66 |
| | very high | Not relevant | 15 | 0.91 | 0.91 | 0.42 | 0.69 | 0.72 | 24 | 0.91 | 0.92 | 0.17 | 0.59 | 0.57 | 61 | 0.93 | 0.95 | 0.42 | 0.38 | 0.56 |


Figure S1. Map of the sampling site (constructed with Google Earth). EC-JRC: European Commission – Joint Research Centre.

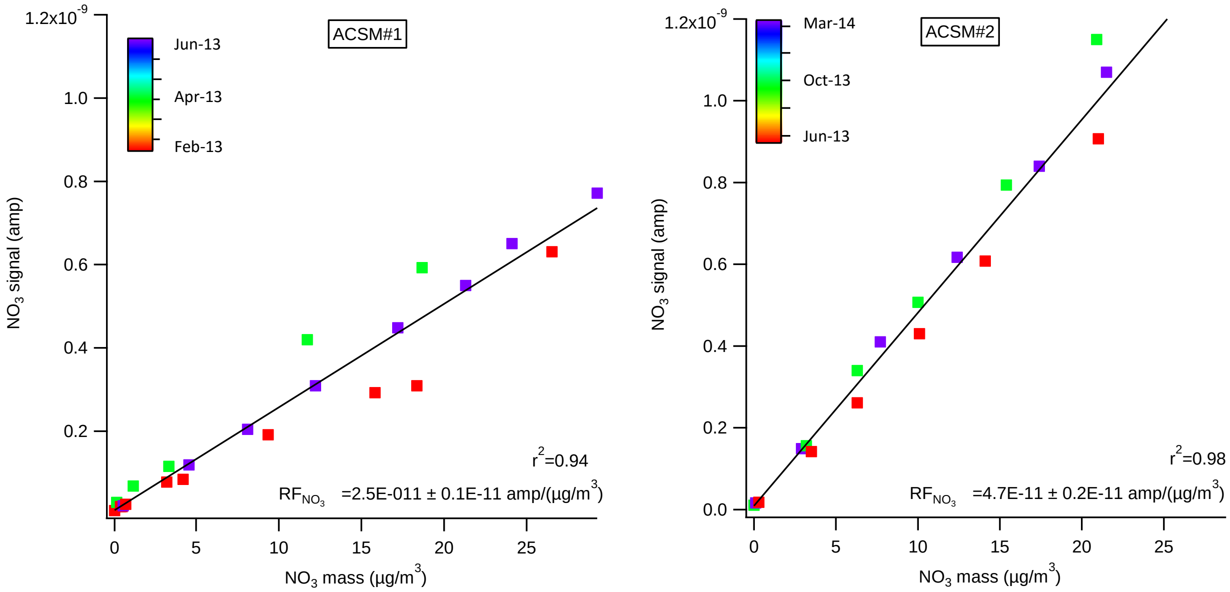


Figure S2. Ammonium nitrate calibrations performed on both ACSMs and colour coded by season. Nitrate response factors ($RF_{NO_3}$) are indicated ± 1 standard error from linear regression. Note that comparable air beam signals were monitored for every calibration: ACSM#1: $(N_2)$signal=1.06E-7 ± 0.04E-7 amp (average ± standard deviation) and ACSM#2: $(N_2)$signal=0.95E-7 ± 0.07E-7 amp; recommended $(N_2)$signal=1.00E-7 amp.

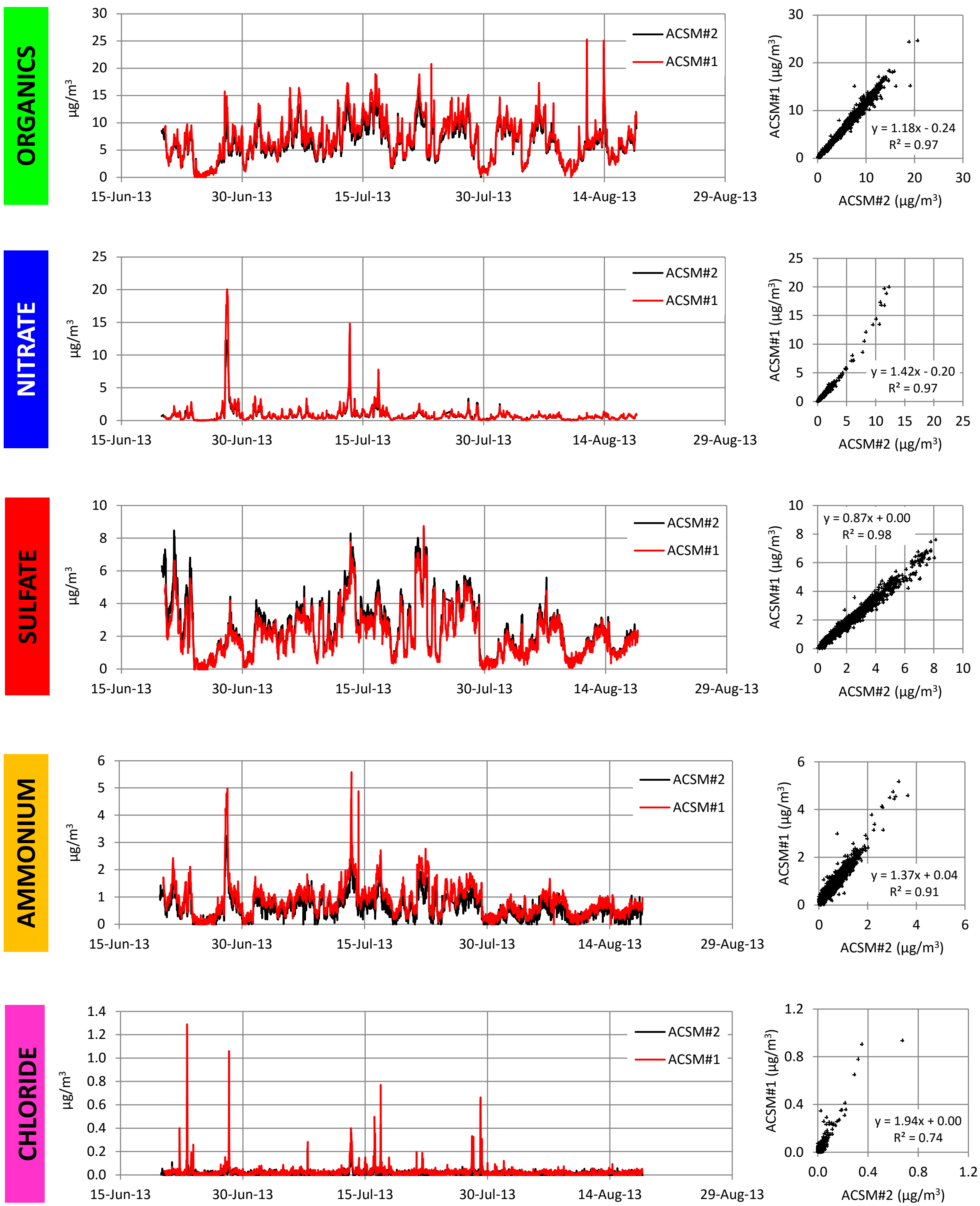


Figure S3. Comparison between two ACSMs for a 2-month summer period. Left panel: time series with 30 min resolution, right panel: scatter plot with 1h time resolution (n=1376, slopes and intercepts are calculated from orthogonal regressions).

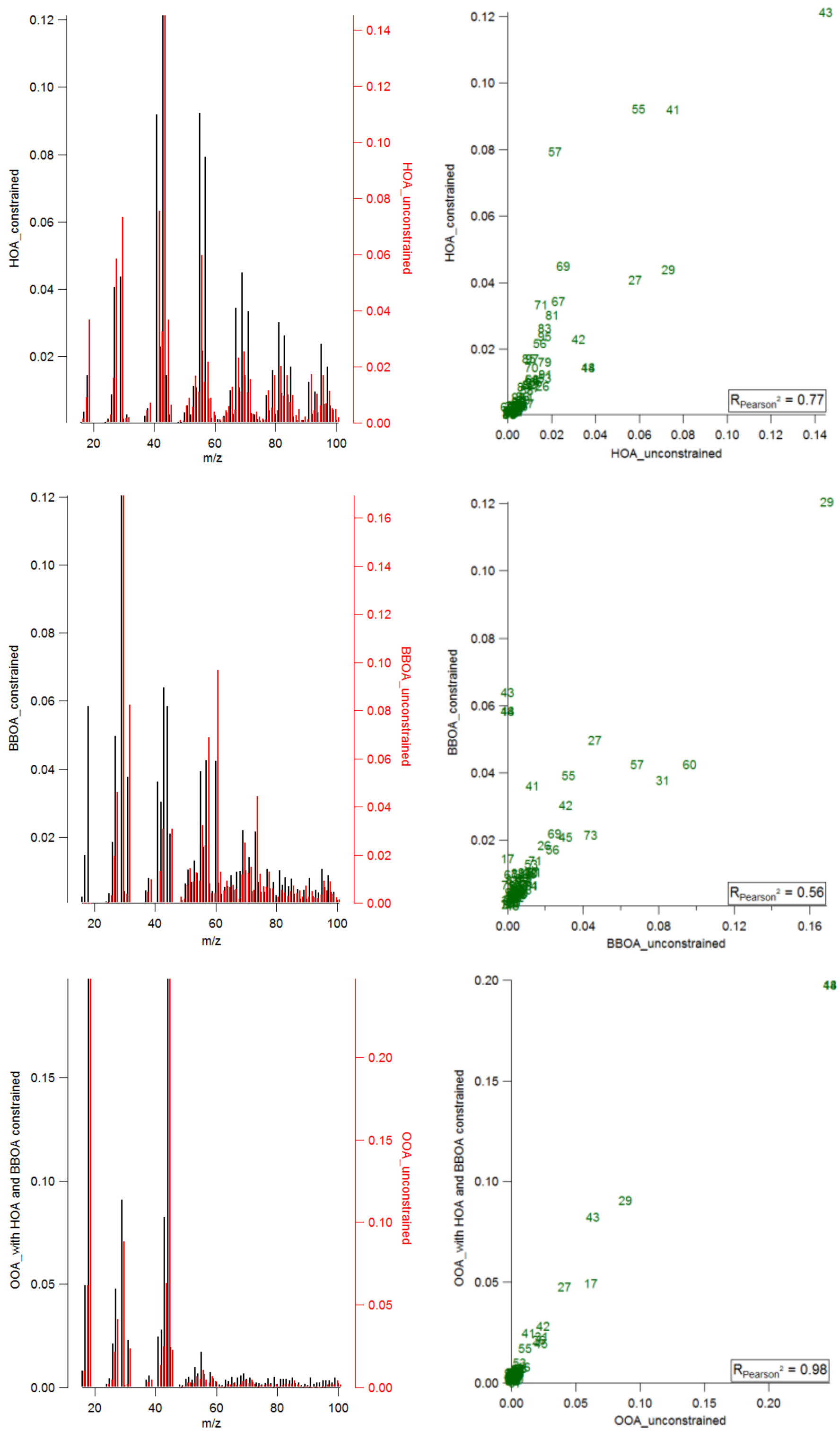

Figure S4. Comparison between constrained and unconstrained factor profiles (spring, three factor solution). Left: relative intensity of every *m/z* in a given factor; right: scatter plots of factor profiles with *m/z* indicated in green.

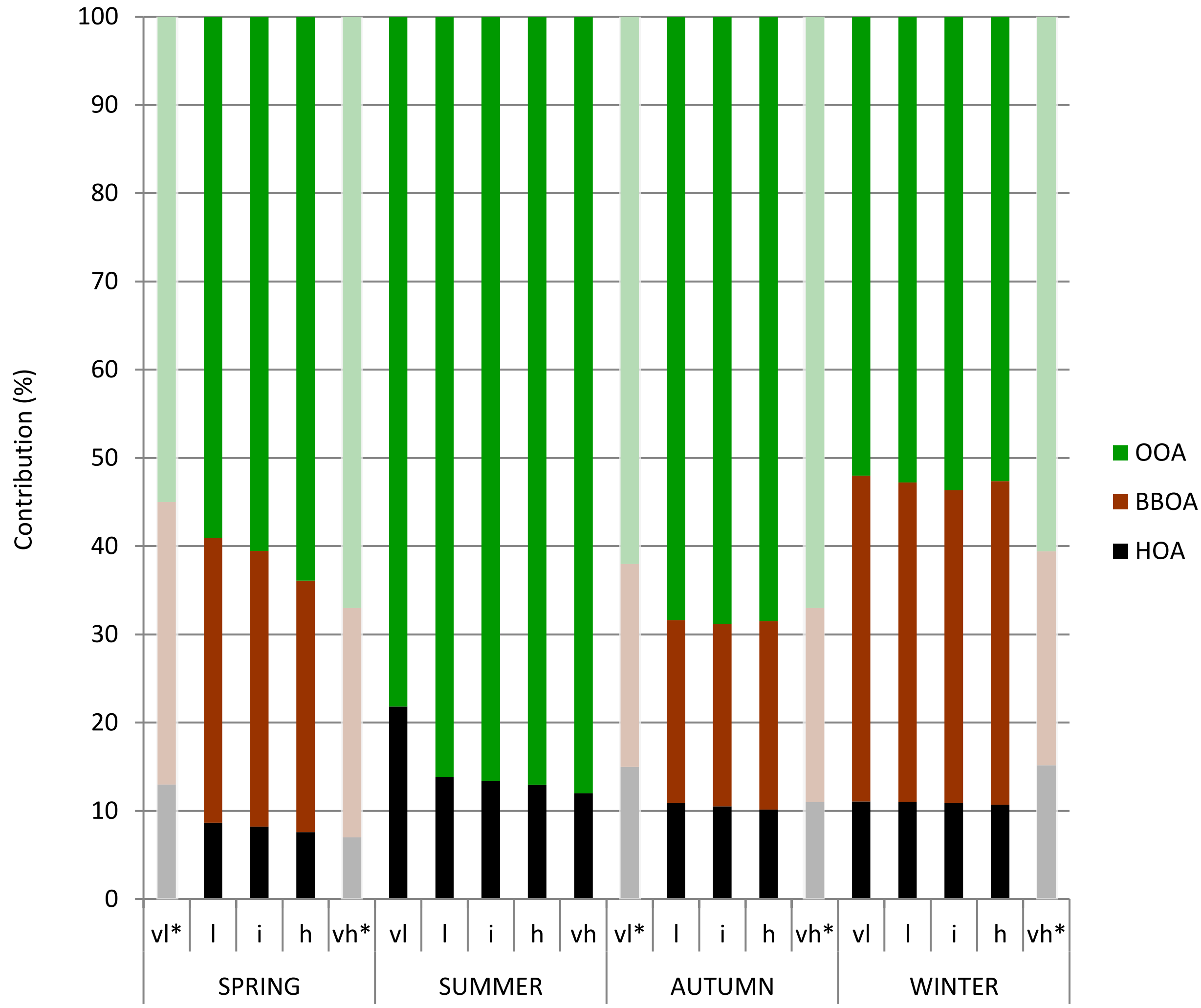


Figure S5. Influence of *α*-values on the average relative contribution of each factor presented by season. vl: very low, l: low, i: intermediate, h: high and vh: very high constraints (see legend Table S2 for more details). Note that scenarios with an asterisk (*) and shaded in grey are regarded as irrelevant due to high seed variability, unexpected daily cycles, etc.

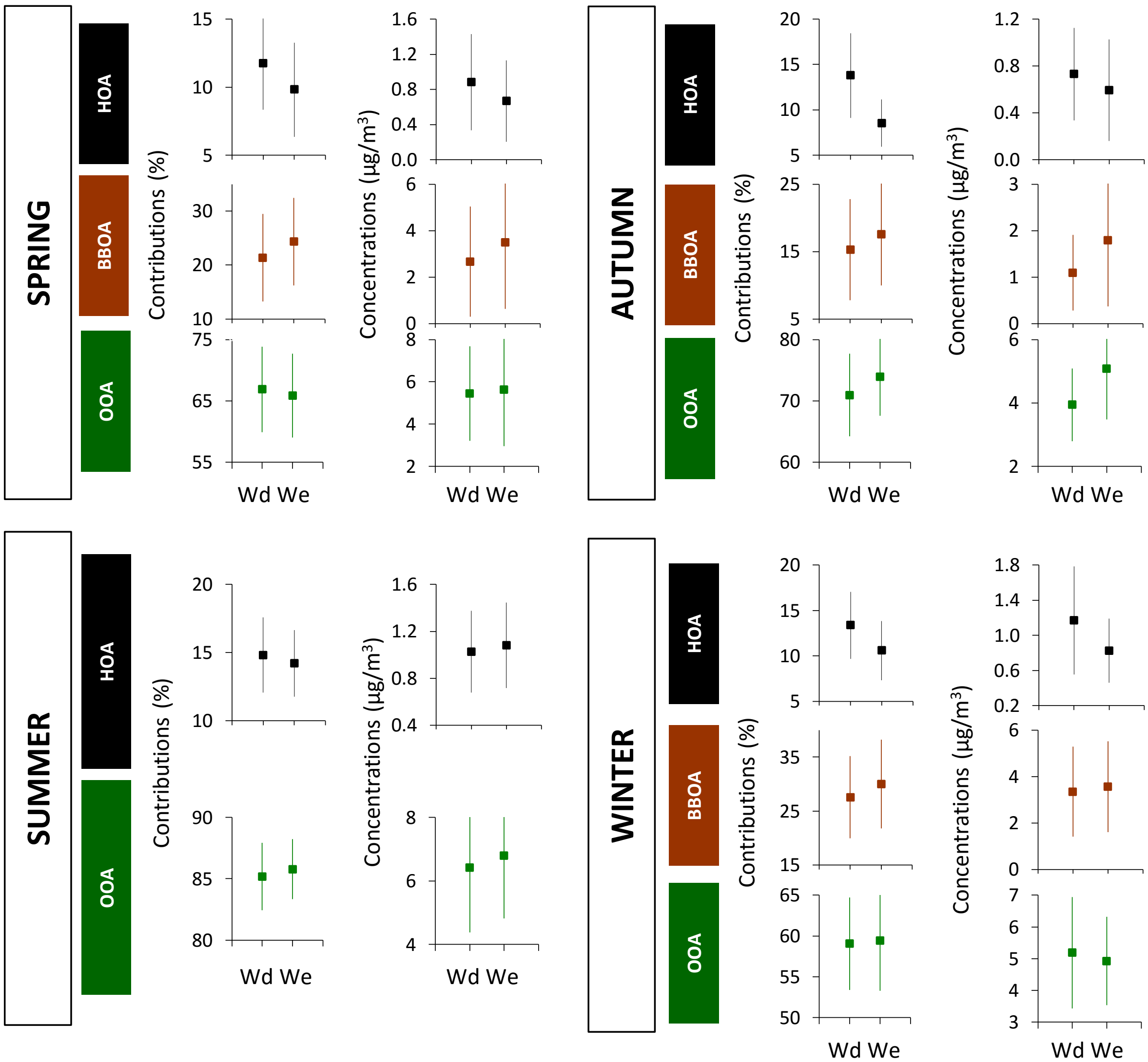


Figure S6. Weekday (Wd) and weekend (We) OA factors contributions (%) and concentrations (µg/m$^3$) for each season. Averages (squares) and 1 standard deviation (error bars) are displayed.

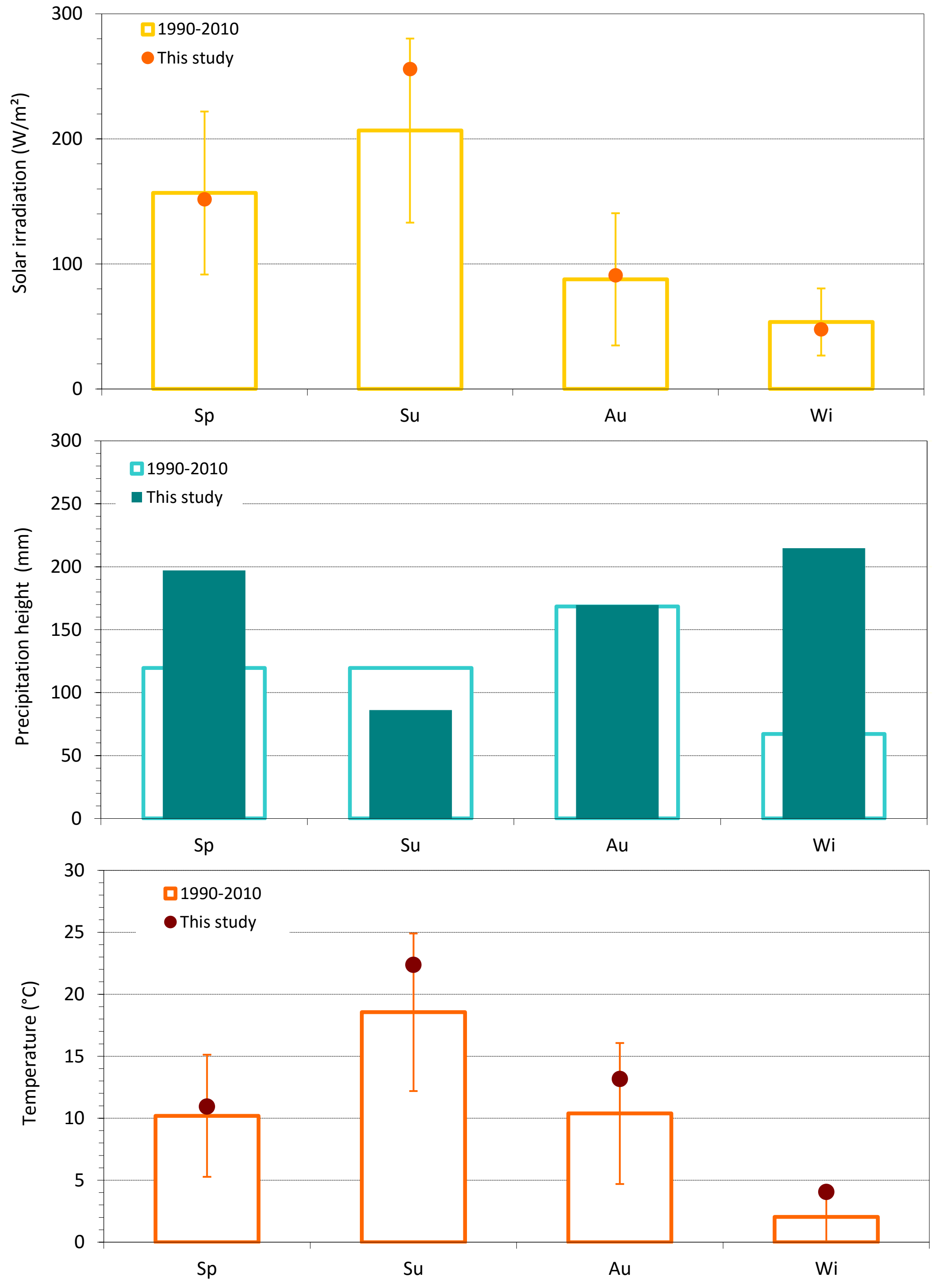


Figure S7. Solar irradiation (top), precipitation height (middle) and temperature (bottom) seasonal averages monitored during this 1-year study, in comparison with the 1990-2010 period averages ± standard deviations measured at the JRC-Ispra site (see Putaud et al., 2014 for more details).

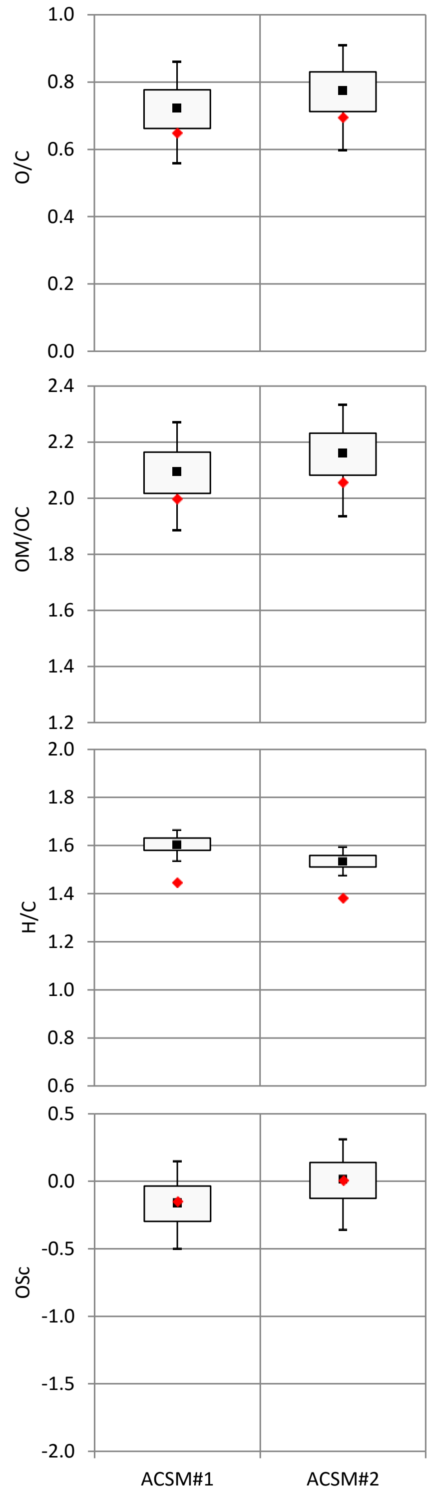


Figure S8. Comparison of O/C, OM/OC, H/C and OSc of ambient OA estimated for ACSM#1 and ACSM#2 from 20 June to 17 August 2013. Black: 5$^{th}$, 25$^{th}$, 50$^{th}$, 75$^{th}$ and 95$^{th}$ percentiles estimates following Canagaratna et al. (2015); red: median estimates following Aiken et al. (2008) for O/C and OM/OC, Ng et al. (2011b) for H/C and Aiken et al. (2008), Kroll et al. (2011) and Ng et al. (2011b) for OSc.

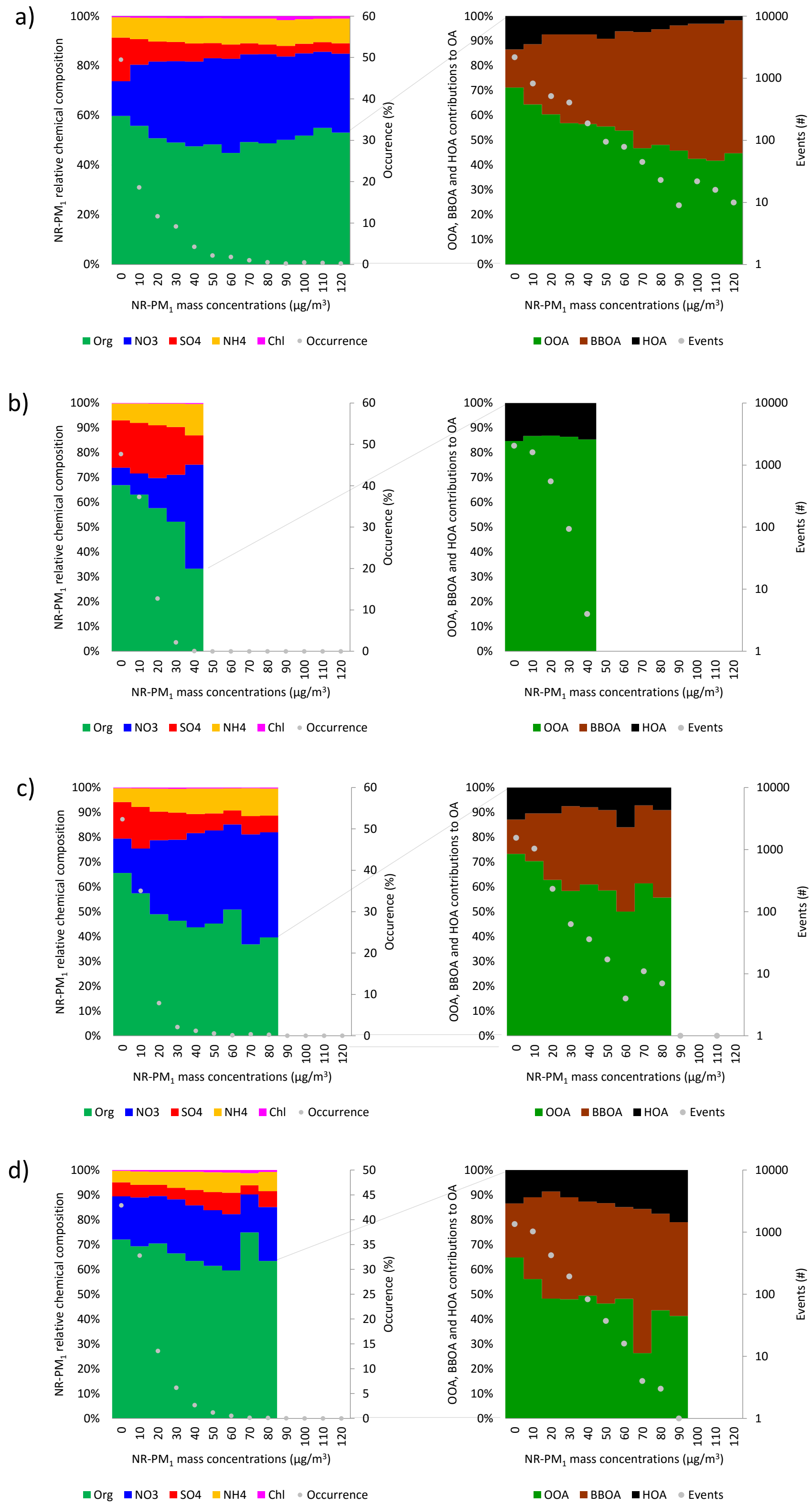


Figure S9. Relative NR-PM$_1$ chemical composition and OA factor contributions as a function of NR-PM$_1$ mass concentrations, for spring (a), summer (b), autumn (c) and winter (d). Only bins with at least 2 pollution events are presented here.

**References**


Aerodyne: Aerosol Chemical Speciation Monitor: Data Analysis Software Manual, available at: ftp://ftp.aerodyne.com/ACSM/ACSM_Manuals/ACSM_Igor_Manual.pdf (last access: 15 February 2016), 2010.

Aerodyne: Application Note AN_014: Using the ACSM Igor $NO_3$ and $SO_4$ calibrations tool, available at: https://sites.google.com/site/ariacsm/mytemplate-documents (last access: 24 November 2014), 2013.

Aiken, A. C., DeCarlo, P. F., Kroll, J. H., Worsnop, D. R., Huffman, J. A., Docherty, K. S., Ulbrich, I. M., Mohr, C., Kimmel, J. R., Sueper, D., Sun, Y., Zhang, Q., Trimborn, A., Northway, M., Ziemann, P. J., Canagaratna, M. R., Onasch, T. B., Alfarra, M. R., Prevot, A. S. H., Dommen, J., Duplissy, J., Metzger, A., Baltensperger, U., and Jimenez, J. L.: O/C and OM/OC ratios of primary, secondary, and ambient organic aerosols with high-resolution time-of-flight aerosol mass spectrometry, Environ. Sci. Technol., 42(12), 4478–4485, doi:10.1021/es703009q, 2008.

Alfarra, M. R., Prevot, A. S. H., Szidat, S., Sandradewi, J., Weimer, S., Lanz, V. A., Schreiber, D., Mohr, M., and Baltensperger, U.: Identification of the mass spectral signature of organic aerosols from wood burning emissions, Environ. Sci. Technol., 41(16), 5770–5777, doi:10.1021/es062289b, 2007.

Allan, J. D., Williams, P. I., Morgan, W. T., Martin, C. L., Flynn, M. J., Lee, J., Nemitz, E., Phillips, G. J., Gallagher, M. W., and Coe, H.: Contributions from transport, solid fuel burning and cooking to primary organic aerosols in two UK cities, Atmos. Chem. Phys., 10(2), 647–668, 2010.

Canagaratna, M. R., Jayne, J. T., Jimenez, J. L., Allan, J. D., Alfarra, M. R., Zhang, Q., Onasch, T. B., Drewnick, F., Coe, H., Middlebrook, A., Delia, A., Williams, L. R., Trimborn, A. M., Northway, M. J., DeCarlo, P. F., Kolb, C. E., Davidovits, P., and Worsnop, D. R.: Chemical and microphysical characterization of ambient aerosols with the aerodyne aerosol mass spectrometer, Mass Spectrom. Rev., 26(2), 185–222, doi:10.1002/mas.20115, 2007.

Canagaratna, M. R., Jimenez, J. L., Kroll, J. H., Chen, Q., Kessler, S. H., Massoli, P., Hildebrandt Ruiz, L., Fortner, E., Williams, L. R., Wilson, K. R., Surratt, J. D., Donahue, N. M., Jayne, J. T., and Worsnop, D. R.: Elemental ratio measurements of organic compounds using aerosol mass spectrometry: characterization, improved calibration, and implications, Atmos. Chem. Phys., 15, 253–272, doi:10.5194/acp-15-253-2015, 2015.

Crenn, V., Sciare, J., Croteau, P. L., Verlhac, S., Fröhlich, R., Belis, C. A., Aas, W., Äijälä, M., Alastuey, A., Artiñano, B., Baisnée, D., Bonnaire, N., Bressi, M., Canagaratna, M., Canonaco, F., Carbone, C., Cavalli, F., Coz, E., Cubison, M. J., Esser-Gietl, J. K., Green, D. C., Gros, V., Heikkinen, L., Herrmann, H., Lunder, C., Minguillón, M. C., Močnik, G., O'Dowd, C. D., Ovadnevaite, J., Petit, J.-E., Petralia, E., Poulain, L., Priestman, M., Riffault, V., Ripoll, A., Sarda-Estève, R., Slowik, J. G., Setyan, A., Wiedensohler, A., Baltensperger, U., Prévôt, A. S. H., Jayne, J. T., and Favez, O.: ACTRIS ACSM intercomparison – part 1: reproducibility of concentration and fragment results from 13 individual quadrupole aerosol chemical speciation monitors (Q-ACSM) and consistency with co-located instruments, Atmos. Meas. Tech., 8(12), 5063–5087, doi:10.5194/amt-8-5063-2015, 2015.

Crippa, M., DeCarlo, P. F., Slowik, J. G., Mohr, C., Heringa, M. F., Chirico, R., Poulain, L., Freutel, F., Sciare, J., Cozic, J., Di Marco, C. F., Elsasser, M., Nicolas, J. B., Marchand, N., Abidi, E., Wiedensohler, A., Drewnick, F., Schneider, J., Borrmann, S., Nemitz, E., Zimmermann, R., Jaffrezo, J.-L., Prévôt, A. S. H., and Baltensperger, U.: Wintertime aerosol chemical composition and source apportionment of the organic fraction in the metropolitan area of Paris, Atmos. Chem. Phys., 13(2), 961–981, doi:10.5194/acp-13-961-2013, 2013.

Crippa, M., Canonaco, F., Lanz, V. A., Äijälä, M., Allan, J. D., Carbone, S., Capes, G., Ceburnis, D., Dall'Osto, M., Day, D. A., DeCarlo, P. F., Ehn, M., Eriksson, A., Freney, E., Hildebrandt Ruiz, L., Hillamo, R., Jimenez, J. L., Junninen, H., Kiendler-Scharr, A., Kortelainen, A.-M., Kulmala, M., Laaksonen, A., Mensah, A. A., Mohr, C., Nemitz, E., O'Dowd, C., Ovadnevaite, J., Pandis, S. N., Petäjä, T., Poulain, L., Saarikoski, S., Sellegri, K., Swietlicki, E., Tiitta, P., Worsnop, D. R., Baltensperger, U., and Prévôt, A. S. H.: Organic aerosol components derived from 25 AMS data sets across Europe using a consistent ME-2 based source apportionment approach, Atmos. Chem. Phys., 14(12), 6159–6176, doi:10.5194/acp-14-6159-2014, 2014.

Dall'Osto, M., Paglione, M., Decesari, S., Facchini, M. C., O'Dowd, C., Plass-Duellmer, C., and Harrison, R. M.: On the Origin of AMS "Cooking Organic Aerosol" at a Rural Site, Environ. Sci. Technol., 49(24), 13964–13972, doi:10.1021/acs.est.5b02922, 2015.

Fröhlich, R., Crenn, V., Setyan, A., Belis, C. A., Canonaco, F., Favez, O., Riffault, V., Slowik, J. G., Aas, W., Aijälä, M., Alastuey, A., Artiñano, B., Bonnaire, N., Bozzetti, C., Bressi, M., Carbone, C., Coz, E., Croteau, P. L., Cubison, M. J., Esser-Gietl, J. K., Green, D. C., Gros, V., Heikkinen, L., Herrmann, H., Jayne, J. T., Lunder, C. R., Minguillón, M. C., Močnik, G., O'Dowd, C. D., Ovadnevaite, J., Petralia, E., Poulain, L., Priestman, M., Ripoll, A., Sarda-Estève, R., Wiedensohler, A., Baltensperger, U., Sciare, J., and Prévôt, A. S. H.: ACTRIS ACSM intercomparison – part 2: intercomparison of ME-2 organic source apportionment results from 15 individual, co-located aerosol mass spectrometers, Atmos. Meas. Tech., 8(6), 2555–2576, doi:10.5194/amt-8-2555-2015, 2015.

Heringa, M. F., DeCarlo, P. F., Chirico, R., Tritscher, T., Dommen, J., Weingartner, E., Richter, R., Wehrle, G., Prévôt, A. S. H., and Baltensperger, U.: Investigations of primary and secondary particulate matter of different wood combustion appliances with a high-resolution time-of-flight aerosol mass spectrometer, Atmos. Chem. Phys., 11(12), 5945–5957, doi:10.5194/acp-11-5945-2011, 2011.

Huang, X.-F., He, L.-Y., Hu, M., Canagaratna, M. R., Sun, Y., Zhang, Q., Zhu, T., Xue, L., Zeng, L.-W., Liu, X.-G., Zhang, Y.-H., Jayne, J. T., Ng, N. L., and Worsnop, D. R.: Highly time-resolved chemical characterization of atmospheric submicron particles during 2008 Beijing Olympic Games using an Aerodyne high-resolution aerosol mass spectrometer, Atmos. Chem. Phys., 10(18), 8933–8945, doi:10.5194/acp-10-8933-2010, 2010.

Kroll, J. H., Donahue, N. M., Jimenez, J. L., Kessler, S. H., Canagaratna, M. R., Wilson, K. R., Altieri, K. E., Mazzoleni, L. R., Wozniak, A. S., Bluhm, H., Mysak, E. R., Smith, J. D., Kolb, C. E., and Worsnop, D. R.: Carbon oxidation state as a metric for describing the chemistry of atmospheric organic aerosol, Nat. Chem., 3(2), 133–139, doi:10.1038/nchem.948, 2011.

Mohr, C., DeCarlo, P. F., Heringa, M. F., Chirico, R., Slowik, J. G., Richter, R., Reche, C., Alastuey, A., Querol, X., Seco, R., Peñuelas, J., Jiménez, J. L., Crippa, M., Zimmermann, R., Baltensperger, U., and Prévôt, A. S. H.: Identification and quantification of organic aerosol from cooking and other sources in Barcelona using aerosol mass spectrometer data, Atmos. Chem. Phys., 12(4), 1649–1665, doi:10.5194/acp-12-1649-2012, 2012.

Ng, N. L., Herndon, S. C., Trimborn, A., Canagaratna, M. R., Croteau, P. L., Onasch, T. B., Sueper, D., Worsnop, D. R., Zhang, Q., Sun, Y. L., and Jayne, J. T.: An aerosol chemical speciation monitor (ACSM) for routine monitoring of the composition and mass concentrations of ambient aerosol, Aerosol Sci. Tech., 45(7), 780–794, doi:10.1080/02786826.2011.560211, 2011a.

Ng, N. L., Canagaratna, M. R., Jimenez, J. L., Zhang, Q., Ulbrich, I. M., and Worsnop, D. R.: Real-time methods for estimating organic component mass concentrations from aerosol mass spectrometer data, Environ. Sci. Technol., 45(3), 910–916, doi:10.1021/es102951k, 2011b.

Putaud, J.-P., Bergamaschi, P., Bressi, M., Cavalli, F., Cescatti, A., Daou, D., Dell'acqua, A., Douglas, K., Duerr, M., Fumagalli, I., Goded Ballarin, I., Grassi, F., Gruening, C., Hjorth, J., Jensen, N., Lagler, F., Manca, G., Martins Dos Santos, S., Matteucci, M., Passarella, R., Pedroni, V., Pokorska, O., and Roux, D.: JRC - Ispra Atmosphere - Biosphere - Climate Integrated monitoring Station 2013 report, EUR - Scientific and Technical Research Reports, Publications Office of the European Union, available at: http://publications.jrc.ec.europa.eu/repository/handle/111111111/33904 (last access: 19 February 2015), 2014.

Sun, Y.-L., Zhang, Q., Schwab, J. J., Demerjian, K. L., Chen, W.-N., Bae, M.-S., Hung, H.-M., Hogrefe, O., Frank, B., Rattigan, O. V., and Lin, Y.-C.: Characterization of the sources and processes of organic and inorganic aerosols in New York City with a high-resolution time-of-flight aerosol mass apectrometer, Atmos. Chem. Phys., 11(4), 1581–1602, doi:10.5194/acp-11-1581-2011, 2011.